J Mol Model (2007) 13: 65–77
DOI 10.1007/s00894-006-0122-2

ORIGINAL PAPER

Vithaya Ruangpornvisuti · Banchob Wanno

Molecular model for host–guest interaction of tetraamino-*tert*-butylthiacalix[4]arene and tetraamino-*tert*-butylcalix[4]arene receptors with carboxylate and dicarboxylate guests: an ONIOM study

Received: 26 April 2005 / Accepted: 3 March 2006 / Published online: 1 June 2006

Abstract Geometry optimizations of tetraamino-*tert*-butylthiacalix[4]arene (tatbtc4a) and tetraamino-*tert*-butylcalix[4]arene (tatbc4a) complexes with acetate, oxalate, malonate, succinate, glutarate, adipate, and pimelate were carried out using the integrated MO:MO method. Thermodynamic quantities, preorganization energies and complexation energies of these complexes were obtained at the ONIOM(B3LYP/6-31G(d):AM1) level of theory. The relative stabilities of the tatbtc4a and tatbc4a complexes with carboxylate guests are reported. The complexes tatbtc4a/malonate and tatbc4a/oxalate were found to be the most stable species. The selectivity of the tatbtc4a receptor toward to malonate with respect to oxalate, in terms of selectivity coefficient, $K^{oxalate}_{malonate}$ is 9.90×10^2.

Keywords Calix[4]arenas · Carboxylate · Host–guest · Recognition · Selectivity · ONIOM

Introduction

Organic anion receptors that contain a chromophore moiety are used for chromogenic sensors for the detection of biological anions. An excellent anion receptor such as thiourea-based chromophores with *p*-nitrophenyl groups is an excellent chromogenic anion receptor for monocarboxylates such as acetate [1]. Anion recognition of two-binding-site receptors led to the discovery of useful sensors, not only for dicarboxylates but also monocarboxylates. Chromogenic azophenol–thiourea-based anion sensors have been developed for the selective colorimetric detection of acetate and other anions [2–4]. Furthermore, chromogenic indoaniline–thiourea-based receptors have been studied for fluoride-detection sensors [5]. Anthracene urea and thiourea compounds have been synthesized and investigated as effective chromogenic anion sensors [6]. Fluorescent and luminescent chemosensors for the detection of anions have been developed for dicarboxylate recognition [7]. The association constants of tripodal urea derivatives such as aromatic carboxylate receptors have been investigated by the NMR titration method [8]. Urea or thiourea groups incorporated in receptors for anion recognition were studied in a system of various solvents [9–11]. In previous theoretical work, the recognition of carboxylate and dicarboxylates by azophenol–thiourea derivatives was first investigated by the integrated MO:MO method and showed that oxalate is the most favorable ion for forming complexes with both receptors of azophenol–thiourea derivatives [12]. Because the determination of the binding and complexation energies of the complexes of the *p*-*tert*-butylsulfonylcalix[4]arene [13], *p*-*tert*-butylthiacalix[4]arene [14], and tetraamino-*tert*-butylthiacalix[4]arene [15] derivatives with zinc(II) cation has been carried out theoretically, the complexes of these receptors with organic anions should also be investigated, particularly calix[4]arene derivatives functionalized by amino groups.

As amino nitrogen atoms of tetraamino-*tert*-butylthiacalix[4]arene derivatives are able to bind to the zinc (II) cations [15, 16], their amino protons must be able to bind anions. As complex formation of tetraamino-*tert*-butylthiacalix[4]arene derivatives with anions is expected and their anion recognition has led to the development of anion sensors, information on the binding interactions between the detected anions and their receptors is very important for discovering colorimetric and other detecting sensors. As organic anions such as acetate, oxalate, malonate, and succinate are important biological anions, detection of these species is very useful for medical and biological purposes. In this work, the binding interactions between carboxylates and different chromophore receptors have therefore been investigated theoretically to obtain their binding energies and thermodynamic data for their interactions. The receptors of tetraamino-*tert*-butylthiacalix[4]arene derivatives and anionic guests of acetate,

V. Ruangpornvisuti (✉) · B. Wanno
Supramolecular Chemistry Research Unit,
Department of Chemistry, Faculty of Science,
Chulalongkorn University,
Bangkok, 10330, Thailand
e-mail: vithaya.r@chula.ac.th
Tel.: +66-2218-7644
Fax: +66-2254-1309

oxalate, malonate, succinate, glutarate, adipate, and pimelate have been investigated in this work.

Computational method

Geometries of the host–guest complexes tested and their host and guest components were optimized using the hybrid density functional B3LYP [17, 18] method and the two-layered ONIOM(MO:MO) approach (ONIOM2) [19, 20] using B3LYP/6-31G(d) as the high-level model and semiempirical AM1 [21], PM3 [22], and MNDO [23] as low-level models. The reliability of the ONIOM2 calculations at the integrated levels [24], ONIOM2(B3LYP/6-31G(d):AM1), ONIOM2(B3LYP/6-31G(d):PM3), and ONIOM2(B3LYP/6-31G(d):MNDO) was examined for geometry optimizations of the tetraamino-*tert*-butylthiacalix[4]arene (tatbtc4a) receptor and its complex with oxalate. Their geometrical data were compared with those of the target geometry optimized at the B3LYP/6-31G(d) level of theory, as listed in Table 1. Energies and geometries of oxalate/tatctb4a system as the host–guest complex were calculated using the ONIOM2(B3LYP/6-31G(d):AM1), ONIOM2(B3LYP/6-31G(d):PM3), and ONIOM2(B3LYP/6-31G(d):MNDO) methods and also compared with the target B3LYP/6-31G(d) geometry. The ONIOM2(B3LYP/6-31G(d):AM1) calculation of the system examined provides reasonable results at a relatively low cost for the present host–guest interactions. The two-layered ONIOM2(B3LYP/6-31G(d):AM1) was therefore used for geometry optimization throughout this work. The reliability of the ONIOM2(B3LYP/6-31G(d):AM1) for a similar system was discussed in the works of Remko et al. [25, 26]. The real and model systems used in the two-layer ONIOM2(MO:MO) calculations for the hosts and host–guest interaction models are shown in Figs. 1 and 2, respectively. The structures of the carboxylate guests and their total energies were optimized and computed at the B3LYP/6-31G(d) level of theory. All calculations were performed using the GAUSSIAN 03 program [27] and their structures were visualized using the MOLEKEL 4.3 program [28].

Energies of binding ($\Delta E_{\text{binding}}$), preorganization ($\Delta E_{\text{preorg.}}$) of host, guest, and complexation ($\Delta E_{\text{complex}}$) of the ONIOM2 calculations of the present system are evaluated using the following formulae:

$$\begin{aligned}\Delta E_{\text{binding}}&\left[\text{ONIOM}\left(\text{B3LYP}/6-31\text{G(d): AM1}\right)\right]\left(\text{host}/\text{guest}\right)\\&=E\left[\text{ONIOM}\left(\text{B3LYP}/6-31\text{G(d): AM1}\right)\right]\left(\text{host}/\text{guest}\right)\\&\quad-E\left[\text{ONIOM}\left(\text{B3LYP}/6-31\text{G(d): AM1}\right)\right](\text{host})\\&\quad-E\left[\text{B3LYP}/6-31\text{G(d)}\right](\text{guest})\end{aligned}\tag{1}$$

$$\begin{aligned}\Delta E_{\text{preorg.}}&(\text{host})\\&=E\left[\text{ONIOM}\left(\text{B3LYP}/6-31\text{G(d): AM1}\right)\right](\text{complexed host})\\&\quad-E\left[\text{ONIOM}\left(\text{B3LYP}/6-31\text{G(d): AM1}\right)\right](\text{isolated host})\end{aligned}\tag{2}$$

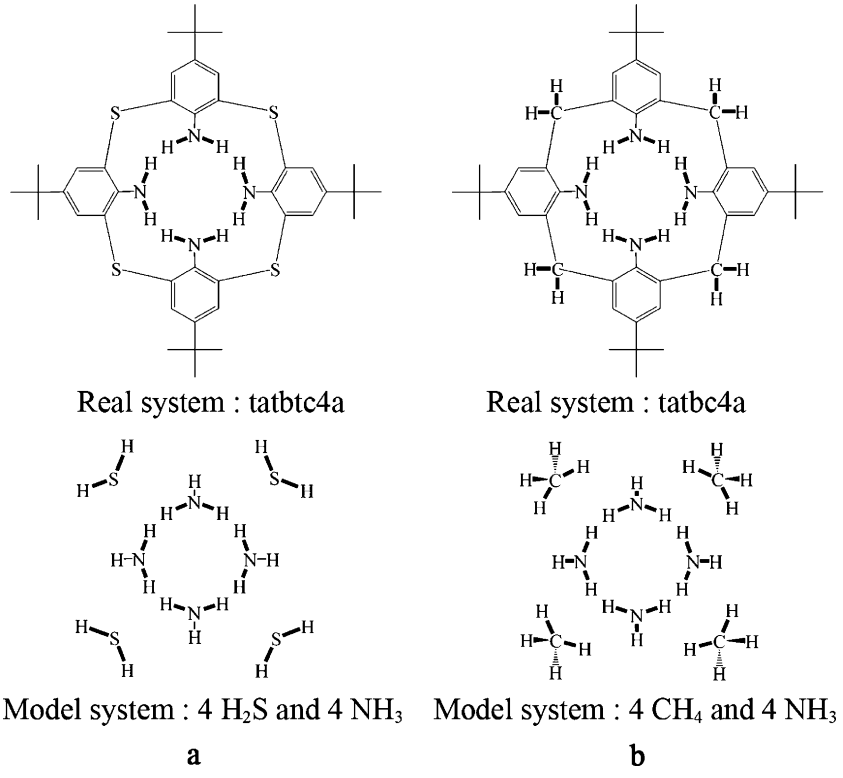

Fig. 1 Real molecule (*top*) and model system (*bottom*) of hosts **a** tatbtc4a and **b** tatca4a. The bold atoms of the real molecules of hosts were treated at the higher level of theory used in the ONIOM(MO:MO) calculation

Table 1 Geometrical data for the geometries of tetraamino-*tert*-butylthiacalix[4]arene (tatbtc4a) complex with oxalate optimized at the B3LYP/6-31G(d), ONIOM(B3LYP/6-31G(d):AM1), ONIOM(B3LYP/6-31G(d):PM3), and ONIOM(B3LYP/6-31G(d):MNDO) levels of theory

Parameter[a]	B3LYP/6-31G(d)	ONIOM (B3LYP/6-31G(d):AM1)	ONIOM (B3LYP/6-31G(d):PM3)	ONIOM (B3LYP/6-31G(d):MNDO)
Host				
Bond distance (Å)				
N1–H1	1.015	1.018	1.040	1.027
N1–H2	1.024	1.031	1.007	1.030
N2–H3	1.011	1.017	1.006	1.027
N2–H4	1.044	1.084	1.040	1.024
N1–C2	1.378	1.406	1.392	1.353
N2–C5	1.333	1.360	1.388	1.360
C1–C2	1.426	1.422	1.425	1.440
C2–C3	1.422	1.419	1.424	1.438
C3–C13	1.397	1.392	1.391	1.400
C13–C14	1.398	1.396	1.390	1.417
C14–C15	1.401	1.400	1.397	1.421
C1–C15	1.392	1.389	1.385	1.398
C14–C16	1.539	1.504	1.513	1.538
C16–C17	1.540	1.524	1.531	1.558
C4–C5	1.439	1.437	1.425	1.435
C5–C6	1.434	1.434	1.426	1.433
C6–C20	1.395	1.385	1.385	1.401
S1–C3	1.815	1.732	1.787	1.731
S1–C4	1.805	1.725	1.787	1.733
S2–C6	1.804	1.724	1.785	1.733
S2–C7	1.816	1.729	1.778	1.732
Bond angle (°)				
H1–N1–H2	107.1	103.9	110.0	107.3
H3–N2–H4	110.0	109.6	110.3	107.1
H5–N3–H6	107.8	106.8	110.8	107.4
H7–N4–H8	110.8	111.6	110.8	107.1
C1–C2–C3	116.1	117.2	118.5	117.9
C3–S1–C4	102.2	99.3	97.5	104.7
C4–C5–C6	115.6	115.8	118.4	118.7
C6–S2–C7	102.2	100.2	101.0	104.6
Dihedral angle (°)				
N1–C2–C3–C13	−173.3	−172.6	−172.9	−163.1
C3–C13–C14–C16	179.0	−179.4	−176.4	175.9
C13–C14–C16–C17	0.2	−1.0	26.0	−5.8
C2–C3–S1–C4	113.7	111.8	93.5	95.6
C3–S1–C4–C5	−88.2	−91.4	−91.5	−107.8
N2–C5–C6–C20	−168.8	−162.5	−173.7	−164.0
C6–C20–C21–C23	177.7	179.7	−176.1	177.3
C20–C21–C23–C24	−1.0	−2.1	−33.2	−10.7
C5–C6–S2–C7	88.8	98.1	114.2	106.0
C6–S2–C7–C8	−116.2	−118.0	−112.0	−95.0
H2–N1–C2–C3	−49.2	−59.1	−6.0	−9.4
H4–N2–C5–C6	−7.4	−28.4	−38.9	−14.7
H6–N3–C8–C9	−22.6	−24.6	−5.6	−9.5
H8–N4–C11–C12	3.5	−22.6	−16.4	−14.7
Guest				
Bond distance (Å)				
C27–C28	1.550	1.553	1.557	1.592
O1–C27	1.241	1.239	1.239	1.264

Table 1 (continued)

Parameter[a]	B3LYP/6-31G(d)	ONIOM (B3LYP/6-31G(d):AM1)	ONIOM (B3LYP/6-31G(d):PM3)	ONIOM (B3LYP/6-31G(d):MNDO)
O2–C27	1.292	1.292	1.294	1.267
O3–C28	1.278	1.288	1.271	1.264
O4–C28	1.268	1.258	1.270	1.268
Bond angle (°)				
O1–C27–O2	126.6	126.9	126.7	125.5
O3–C28–O4	125.7	125.3	126.8	125.5
Dihedral angle (°)				
O1–C27–C28–O3	96.1	93.9	90.6	−176.4
Host/guest				
Bond distance (Å)[b]				
N2–H4...O4	1.706	1.566	1.994	1.994
N1–H2...O3	1.981	2.039	2.376	2.376
N3–H6...O2	1.905	1.856	2.013	2.013
N4–H7...O2	1.726	1.732	1.980	1.980

[a]Atomic labeling is shown in Fig. 2
[b]Hydrogen bond

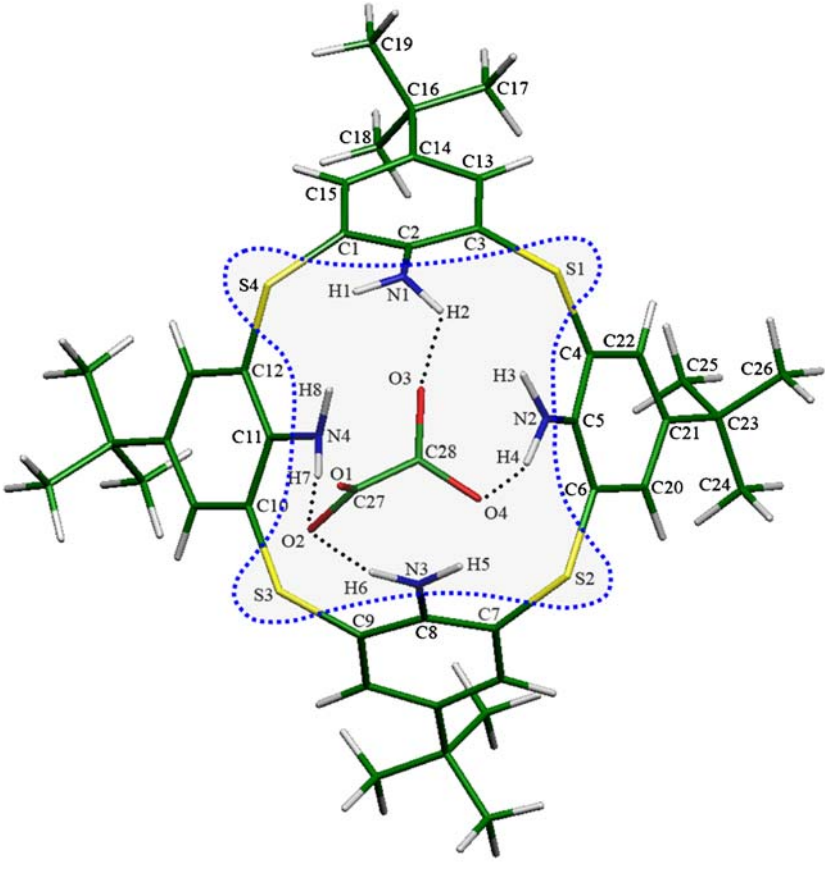

Fig. 2 Atom labeling of tatbt-c4a/oxalate complex as a representative of a host–guest system

$$\Delta E_{\text{preorg.}}(\text{guest}) = E\left[\text{B3LYP}/6-31\text{G(d)}\right](\text{complexed guest}) - E\left[\text{B3LYP}/6-31\text{G(d)}\right](\text{isolated guest}) \quad (3)$$

$$\Delta E_{\text{complex}} = E\left[\text{ONIOM}\left(\text{B3LYP}/6-31\text{G(d)}:\text{AM1}\right)\right](\text{host/guest}) - E\left[\text{ONIOM}\left(\text{B3LYP}/6-31\text{G(d)}:\text{AM1}\right)\right](\text{complexed host}) - E\left[\text{B3LYP}/6-31\text{G(d)}\right](\text{complexed guest}) \quad (4)$$

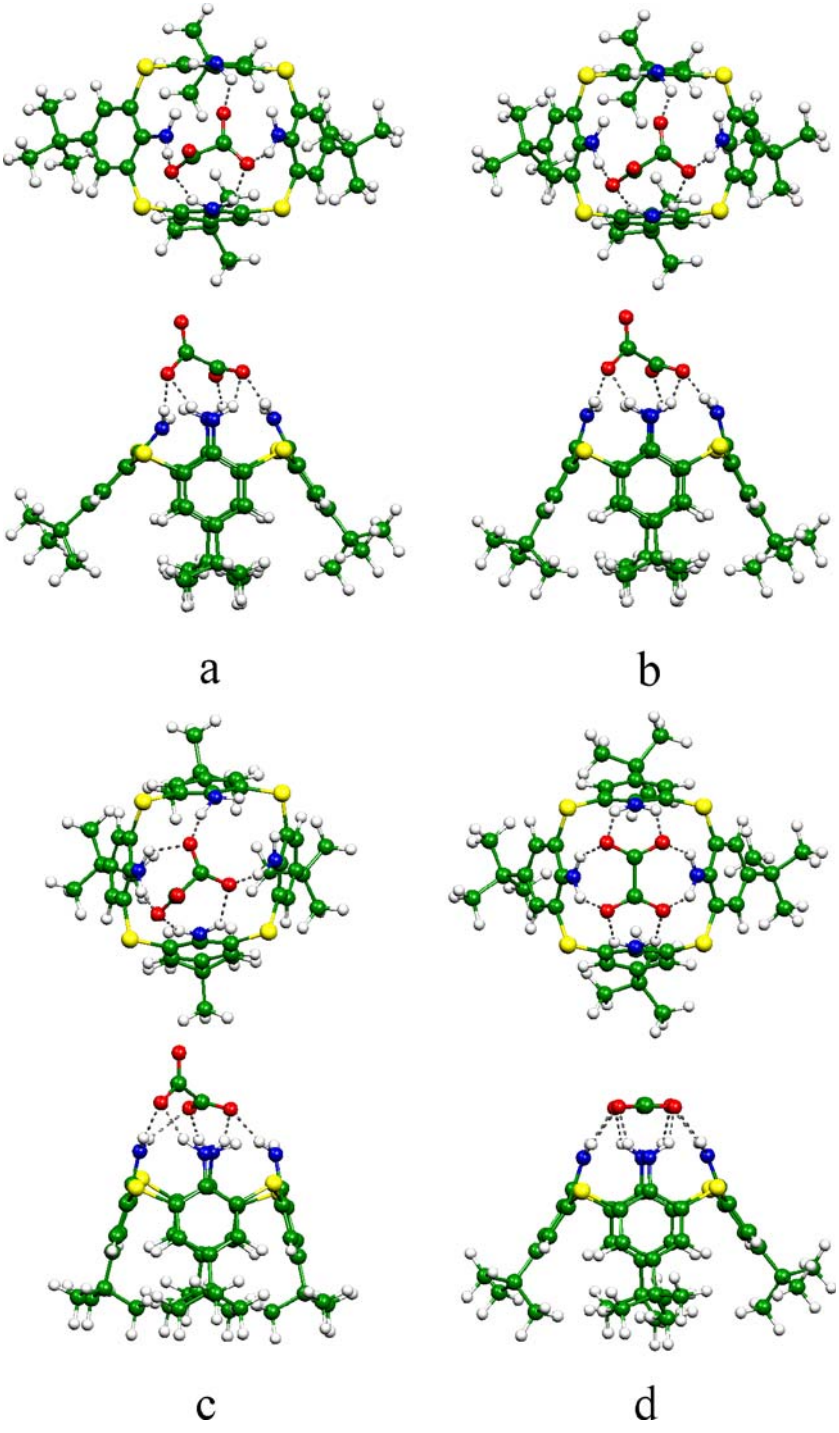

Fig. 3 Geometrical structures of tetraamino-*tert*-butylthiacalix[4]arene (tatbtc4a) complex with oxalate optimized at **a** B3LYP/6-31G, **b** ONIOM (B3LYP/6-31G(d):AM1), **c** ONIOM(B3LYP/6-31G(d):PM3), and **d** ONIOM(B3LYP/6-31G(d):MNDO) levels of theory

Table 2 Binding energies, enthalpies, and free energies of association of tetraamino-*tert*-butylthiacalix[4]arene (tatbtc4a) and various anionic guests

Guest	$\Delta E_{\text{binding}}$[a]	ΔH^{298}[a]	ΔG^{298}[a]	K_B^{acetate}[b]
Acetate	−43.32	−43.61	−28.03	1.00×10^{00}
Oxalate	−103.77	−104.26	−80.92	8.12×10^{38}
Malonate	−117.60	−41.35	−84.99	8.04×10^{41}
Succinate	−86.91	−87.71	−68.80	9.83×10^{29}
Glutarate	−75.06	−75.64	−58.19	1.54×10^{22}
Adipate	−4.93	_[c]	_[c]	_[d]
Pimelate	−58.98	−60.26	−42.38	3.62×10^{10}

[a]In kcal mol^{-1}, derived from the ONIOM(B3LYP/6-31G(d):AM1) energies with ZPVE corrections
[b]Selectivity coefficient of guests with respect to acetate
[c]Unreliable results due to the ONIOM(B3LYP/6-31G(d):AM1) frequency calculations
[d]Indetermination

$$\Delta E_{binding} = \Delta E_{\text{preorg.}}(\text{host}) + \Delta E_{\text{preorg.}}(\text{guest}) + \Delta E_{\text{complex}} \quad (5)$$

$$\Delta E^{total}_{preorg.} = \Delta E_{binding} - \Delta E_{complex} \quad (6)$$

To estimate the basis set superposition error (BSSE) in the energies of host/guest complex formation at the B3LYP/6-31G(d)//ONIOM2(B3LYP/6-31G(d):AM1) level, counterpoise (CP) calculations were performed using the Boys–Bernardi CP scheme [29–34]. The BSSE energies of host/guest complex formation were used to compute the energies of BSSE-corrected binding $\left(\Delta E^{BSSE}_{binding.}\right)$ and complexation $\left(\Delta E^{BSSE}_{complex.}\right)$. The total preorganization

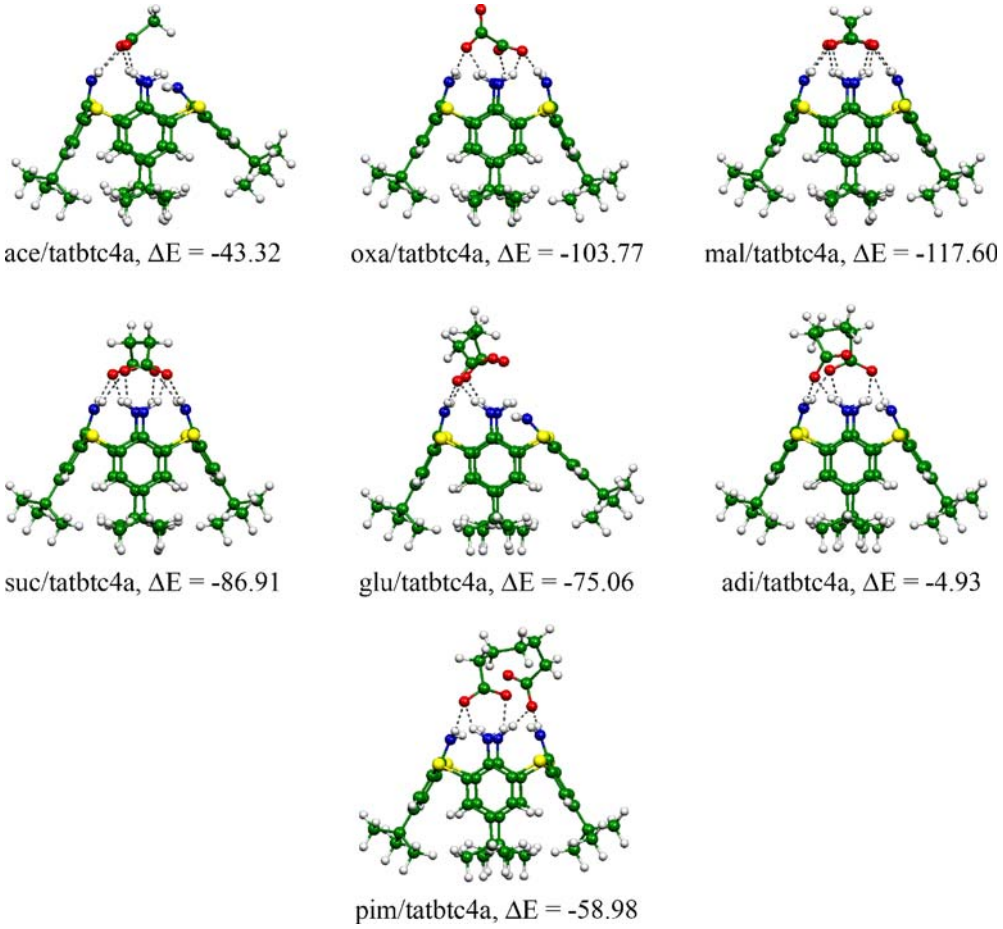

Fig. 4 ONIOM(B3LYP/6-31G(d):AM1)-optimized geometries of tetraamino-*tert*-butylthiacalix[4]arene (tatbtc4a) with carboxylate guests. Binding energies ΔE are in kilocalorie per mole

Table 3 Preorganization energies, corresponding thermodynamics of tatbtc4a receptor (host), carboxylates (guest), and their complexation energies derived from the ONIOM (B3LYP/6-31G(d):AM1) calculations

Host/guest	Host			Guest			$\Delta E^{\text{total}}_{\text{preorg.}}$ [a]	$\Delta E_{\text{complex}}$ [a]
	$\Delta E^{\text{host}}_{\text{preorg.}}$ [a]	ΔH^{298a}	ΔG^{298a}	$\Delta E^{\text{guest}}_{\text{preorg.}}$ [b]	ΔH^{298b}	ΔG^{298b}		
tatbtc4a/acetate	10.65	10.67	10.99	0.86	0.26	2.79	11.51	−54.83
tatbtc4a/oxalate	22.54	21.56	25.01	1.54	1.03	8.66	24.08	−127.85
tatbtc4a/malonate	1.84	1.53	2.10	2.47	64.59	3.81	4.31	−138.72
tatbtc4a/succinate	18.06	16.55	22.32	13.07	12.91	13.69	31.13	−118.04
tatbtc4a/glutarate	17.75	16.31	20.27	17.05	15.87	19.24	34.8	−109.86
tatbtc4a/adipate	17.54	16.74	19.03	83.28	83.02	85.53	100.82	−105.75
tatbtc4a/pimelate	17.87	17.04	19.85	26.49	25.00	27.93	44.36	−103.34

[a]In kcal mol^{-1}, derived at the ONIOM (B3LYP/6-31G(d):AM1) level with ZPVE corrections
[b]In kcal mol^{-1}, derived at the B3LYP/6-31G(d) level with ZPVE corrections

energy with BSSE correction $\left(\Delta E^{BSSE}_{preorg.}\right)$ was therefore evaluated using Eq. 7.

$$\Delta E^{BSSE}_{preorg.} = \Delta E^{BSSE}_{binding.} - \Delta E^{BSSE}_{complex.} \tag{7}$$

The enthalpy ΔH^{298} and Gibbs free energy changes ΔG^{298} of all complexation reactions were derived from frequency calculation at the ONIOM(B3LYP/6-31G(d): AM1) level of theory. The equilibrium constant, K of the binding process at 298.15 and 1 atmosphere was computed using the thermodynamic relation ΔG^{298}=−RT ln K.

The binding selectivity of calix[4]arene receptor to guest B with respect to guest A was derived from the selectivity coefficient K^A_B, [35] which is defined as an equilibrium constant for ion exchange between ions A and B. Because exchange is a chemical reaction, Eq. 8, it can be treated like any other mass-action expression.

$$\mathrm{AX} + \mathrm{B} \rightleftharpoons \mathrm{BX} + \mathrm{A} \tag{8}$$

Therefore, the selectivity coefficient can be defined as $K^A_B = \frac{[\mathrm{BX}][\mathrm{A}]}{[\mathrm{AX}][\mathrm{B}]}$. If complexation of BX and AX are observed, their stability constants according to Eqs. (9 and 10) can be expressed as $K_A = \frac{[\mathrm{AX}]}{[\mathrm{X}][\mathrm{A}]}$ and $K_B = \frac{[\mathrm{BX}]}{[\mathrm{X}][\mathrm{B}]}$.

$$\mathrm{X} + \mathrm{B} \rightleftharpoons \mathrm{BX} \tag{9}$$

$$\mathrm{X} + \mathrm{A} \rightleftharpoons \mathrm{AX} \tag{10}$$

The selectivity coefficient can be therefore written as $K^A_B = \frac{K_B}{K_A}$. If the value of the selectivity coefficient K^A_B is larger than one, this implies that B is preferred over A and if K^A_B is smaller than one, A is preferred over B.

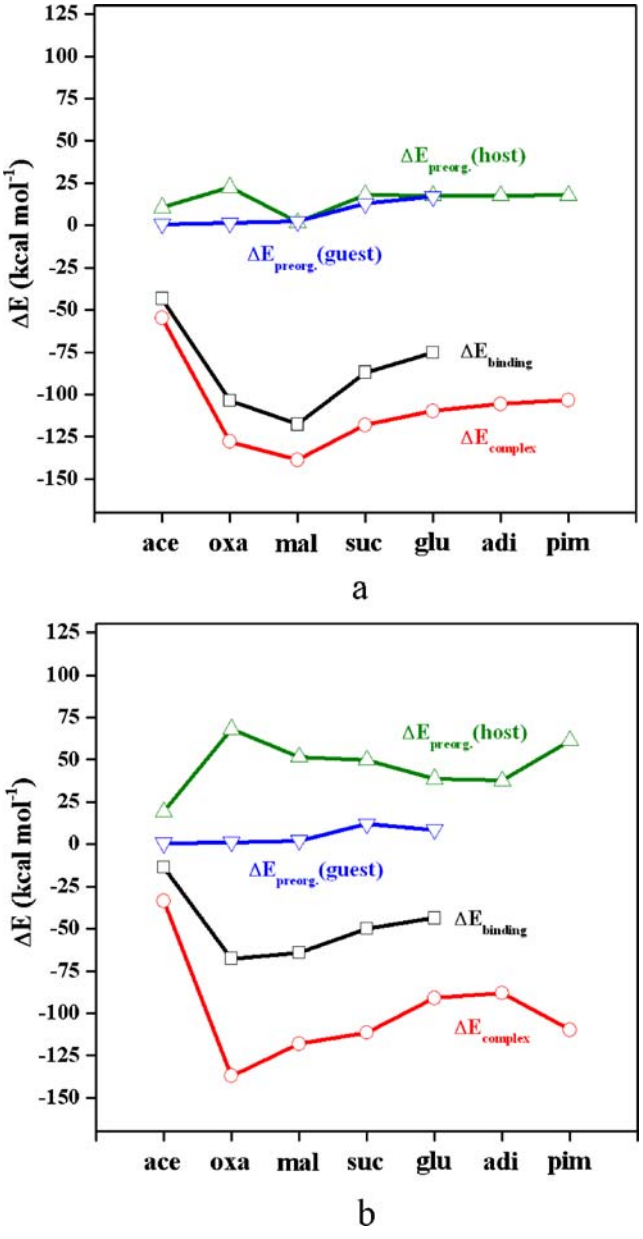

Fig. 5 Plots of preorganization energies of **a** tatbtc4a receptor and carboxylates (guests) and **b** tatbc4a receptor and carboxylates (guests) and their complexation and binding energies against the size of the carboxylate guests, based on the ONIOM(B3LYP/6-31G(d):AM1) method

Table 4 Binding energies of association of the tetraamino-*tert*-butylthiacalix[4]arene (tatbtc4a) and various anionic guests and their BSSE corrections values derived from the B3LYP/6-31G(d)//ONIOM (B3LYP/6-31G(d):AM1) calculations and their BSSE corrected values

Host/guest	$\Delta E_{binding}$ [a]	$\Delta E_{complex}$ [a]	BSSE[a,b]	$\Delta E^{BSSE}_{binding.}$ [a]	$\Delta E^{BSSE}_{complex.}$ [a]	$\Delta E^{BSSE}_{preorg.}$ [a]
tatbtc4a/acetate	−45.35	−86.82	–[c]	–	–	–
tatbtc4a/oxalate	−98.07	−209.13	31.92	−66.16	−177.22	111.06
tatbtc4a/malonate	−100.16	−210.84	31.37	−68.79	−179.47	110.68
tatbtc4a/succinate	−83.33	−204.17	31.54	−51.79	−172.63	120.84
tatbtc4a/glutarate	−67.54	−191.06	24.94	−42.60	−166.12	123.52
tatbtc4a/adipate	−61.70	−189.21	–[d]	–	–	–
tatbtc4a/pimelate	–[e]	–[e]	13.69	–[f]	–[f]	132.50

[a]In kcal mol^{-1}
[b]The BSSE energy
[c]No convergence
[d]Unreliable results
[e]No convergence of energies
[f]Indetermination

Results and discussion

To examine the reliability of the two-layered ONIOM2 (MO:MO) method, the geometries of the tatbtc4a/oxalate complex were optimized at four different levels of theory. Its geometries optimized at the B3LYP/6-31G(d), ONIOM2(B3LYP/6-31G(d):AM1), ONIOM2(B3LYP/6-31G(d):PM3), and ONIOM2(B3LYP/6-31G(d):MNDO) levels of theory are shown in Fig. 3 and their corresponding geometrical data are given in Table 1. Comparing the hydrogen bonds of the tatbtc/oxalate complex shown that the ONIOM2(B3LYP/6-31G(d):AM1)-optimized hydrogen-bond distances are in good agreement with the B3LYP/6-31G(d)-optimized data (see Table 1). The ONIOM2(B3LYP/6-31G(d):AM1)-optimized geometry of the tatbtc/oxalate complex is very similar to the target B3LYP/6-31G(d)-optimized geometry (Fig. 3, see Table 1). Thus, the reliability test of the ONIOM2(MO:MO) approach for this host–guest system showed the ONIOM2(B3LYP/6-31G(d):AM1) method to be the most reliable with respect to the full B3LYP/6-31G(d) level of theory.

Complexation of tetraamino-*tert*-butylthiacalix[4] arene (tatbtc4a)

Tetraamino-*tert*-butylthiacalix[4]arene (tatbtc4a) can form stable complexes with acetate, oxalate, malonate, succinate, glutarate, and pimelate guests, but not with adipate. The most stable complex is that with malonate, which is stabilized by −117.60 kcal mol^{-1}. The stability of the tatbtc4a/carboxylate complex system in decreasing order is malonate > oxalate > succinate > pimelate > glutarate > acetate (see Table 2). The ONIOM(B3LYP/6-31G(d):AM1)-optimized geometries of the tatbtc4a complexes with carboxylate guests are shown in Fig. 4. The geometries of malonate/tatbtc4a and succinate/tatbtc4a are found to have high symmetry, belonging to the point group C_2 (see Fig. 4). The selectivity coefficient of the tatbtc4a towards malonate with respect to acetate also confirms that the tatbtc4a favorably forms a very stable complex with malonate. As the selectivity coefficient of tatbtc4a toward malonate with respect to oxalate (the second most stable complex with tatbtc4a), $K^{oxalate}_{malonate}$ is quite large (9.90×10^2), the receptor tatbtc4a may well recognize malonate. Table 3 shows that the total pre-organization energy of the host tatbtc4a ($\Delta E^{host}_{preorg.}$ = 1.84 kcal mol^{-1}) and the guest malonate ($\Delta E^{guest}_{preorg.}$ = 3.81 kcal mol^{-1}) are smallest ($\Delta E^{total}_{preorg.}$ =4.31 kcal mol^{-1}). The largest guest-preorganization energy is given by adipate ($\Delta E^{guest}_{preorg.}$ =83.28 kcal mol^{-1}). Plots of the preorganization energies of tatbtc4a, its complexation, and binding energies against the size of the carboxylate guests, based on the ONIOM(B3LYP/6-31G(d):AM1) method, are shown in Fig. 5a. Binding energies with and without BSSE corrections, BSSE-corrected preorganization energies of the association of the tetraamino-*tert*-butylthiacalix[4]arene (tatbtc4a), and various anionic guests derived at the B3LYP/6-31G(d)//ONIOM (B3LYP/6-31G(d):AM1) level of theory are shown in

Table 5 Binding energies, enthalpies, and free energies of association of tetraamino-*tert*-butylcalix[4]arene (tatbc4a) and various anionic guests

Guest	$\Delta E_{binding}$ [a]	ΔH^{298a}	ΔG^{298a}	$K_B^{acetate}$ [b]
Acetate	−13.60	−8.28	−7.73	1.00×10^{00}
Oxalate	−67.61	−62.58	−54.28	1.76×10^{34}
Malonate	−64.09	–[c]	–[c]	–[d]
Succinate	−49.77	−44.56	−42.66	5.00×10^{25}
Glutarate	−43.71	−39.01	−36.58	1.69×10^{21}
Adipate	25.78[e]	–[c]	–[c]	–[d]
Pimelate	−26.72	−22.79	−18.41	7.27×10^{7}

[a]In kcal mol^{-1}, derived from the ONIOM (B3LYP/6-31G(d):AM1) energies with ZPVE corrections
[b]Selectivity coefficient of guests with respect to acetate
[c]Unreliable results due to the ONIOM (B3LYP/6-31G(d):AM1) frequency calculations
[d]Indetermination
[e]Destabilized complex

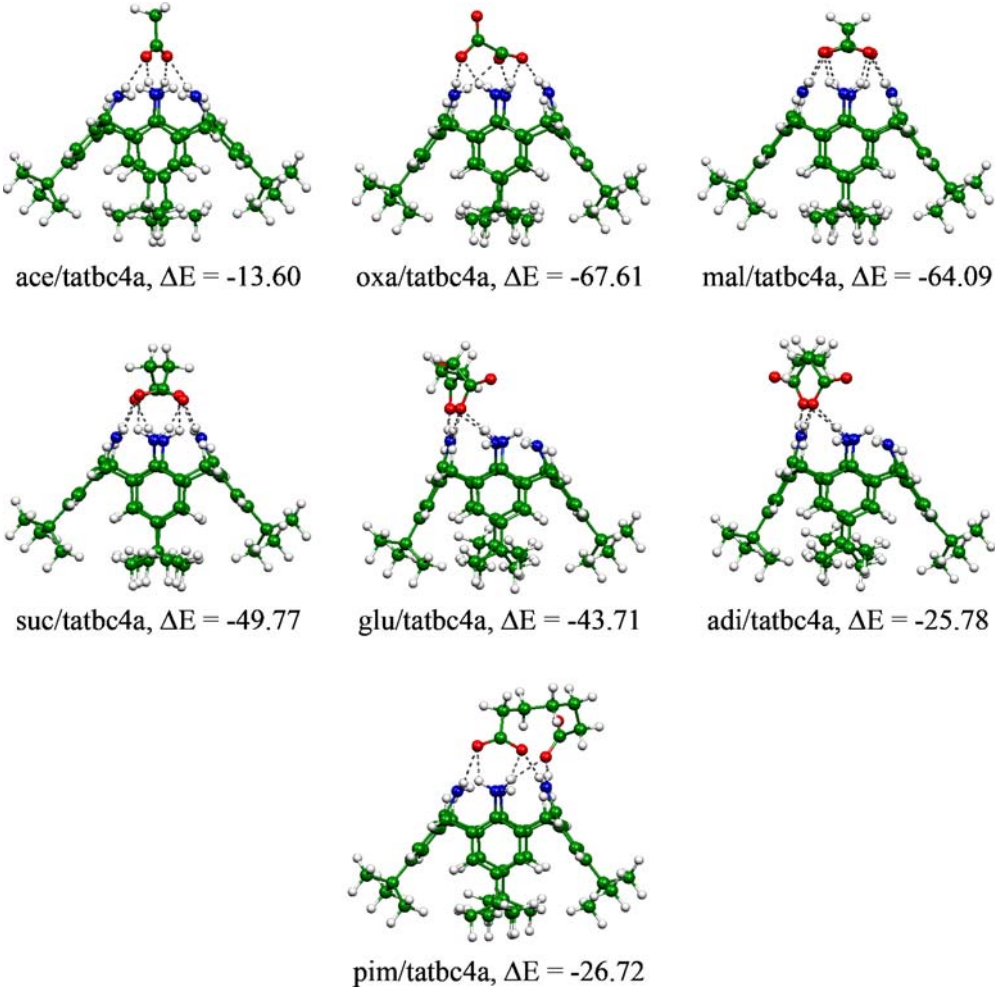

Fig. 6 ONIOM(B3LYP/6-31G (d):AM1)-optimized geometries of tetraamino-*tert*-butylcalix[4]arene (tatbc4a) with carboxylate guests. Binding energies ΔE are in kilocalorie per mole

Table 4. The binding energies with and without the BSSE corrections indicate that the tatbtc4a/malonate complex is the most stable species with the lowest BSSE-corrected preorganization energy (110.68 kcal mol^{-1}).

Complexation of tetraamino-*tert*-butylcalix[4]arene (tatbc4a)

Tetraamino-*tert*-butylcalix[4]arene (tatbc4a) forms stable complexes with oxalate, malonate, succinate, and glutarate, and weak complexes with acetate and pimelate, as indicated by the binding and Gibbs free energies shown in Table 5. The most stable complex is that with oxalate,

Table 6 Preorganization energies, corresponding thermodynamics of tatbc4a receptor (host), carboxylates (guest), and their complexation energies derived from the ONIOM (B3LYP/6-31G(d):AM1) calculations

Host/guest	Host			Guest			$\Delta E_{\text{preorg.}}^{\text{total}}$ [a]	$\Delta E_{\text{complex}}$ [a]
	$\Delta E_{\text{preorg.}}^{\text{host}}$ [a]	ΔH^{298a}	ΔG^{298a}	$\Delta E_{\text{preorg.}}^{\text{guest}}$ [b]	ΔH^{298b}	ΔG^{298b}		
tatbc4a/acetate	19.27	18.64	19.96	0.67	0.08	2.61	19.94	−33.54
tatbc4a/oxalate	68.05	71.96	62.11	1.31	0.80	8.44	69.36	−136.98
tatbc4a/malonate	51.76	55.83	44.66	2.19	64.31	3.52	53.95	−118.04
tatbc4a/succinate	49.79	54.49	41.22	11.97	11.82	12.48	61.76	−111.53
tatbc4a/glutarate	38.64	43.21	31.02	8.60	7.44	10.81	47.24	−90.95
tatbc4a/adipate	37.62	42.23	30.03	76.28	75.10	79.97	113.9	−88.13
tatbc4a/pimelate	61.35	65.27	55.77	21.83	19.78	24.21	83.18	−109.89

[a]In kcal mol^{-1}, derived at the ONIOM (B3LYP/6-31G(d):AM1) level with ZPVE corrections
[b]In kcal mol^{-1}, derived at the B3LYP/6-31G(d) level with ZPVE corrections

Table 7 Binding energies of association of the tetraamino-*tert*-butylcalix[4]arene (tatbc4a) and various anionic guests and their BSSE corrections values derived from the B3LYP/6-31G(d)//ONIOM (B3LYP/6-31G(d):AM1) calculations and their BSSE corrected values

Host/guest	$\Delta E_{binding}$ [a]	$\Delta E_{complex}$ [a]	BSSE[a,b]	$\Delta E^{BSSE}_{binding.}$ [a]	$\Delta E^{BSSE}_{complex.}$ [a]	$\Delta E^{BSSE}_{preorg.}$ [a]
tatbc4a/acetate	−34.10	−85.60	–[c]	–	–	–
tatbc4a/oxalate	−93.17	−240.76	31.92	−61.26	−208.84	147.59
tatbc4a/malonate	−91.53	−246.99	47.97	−43.56	−199.02	155.46
tatbc4a/succinate	−77.36	−243.25	50.25	−27.11	−193.00	165.90
tatbc4a/glutarate	−70.55	−208.86	34.18	−36.38	−174.68	138.30
tatbc4a/adipate	−64.15	−206.13	34.81	−29.34	−171.32	141.98
tatbc4a/pimelate	−54.41	−213.32	43.75	−10.66	−169.57	158.91

[a]In kcal mol^{-1}
[b]The BSSE energy
[c]No convergence

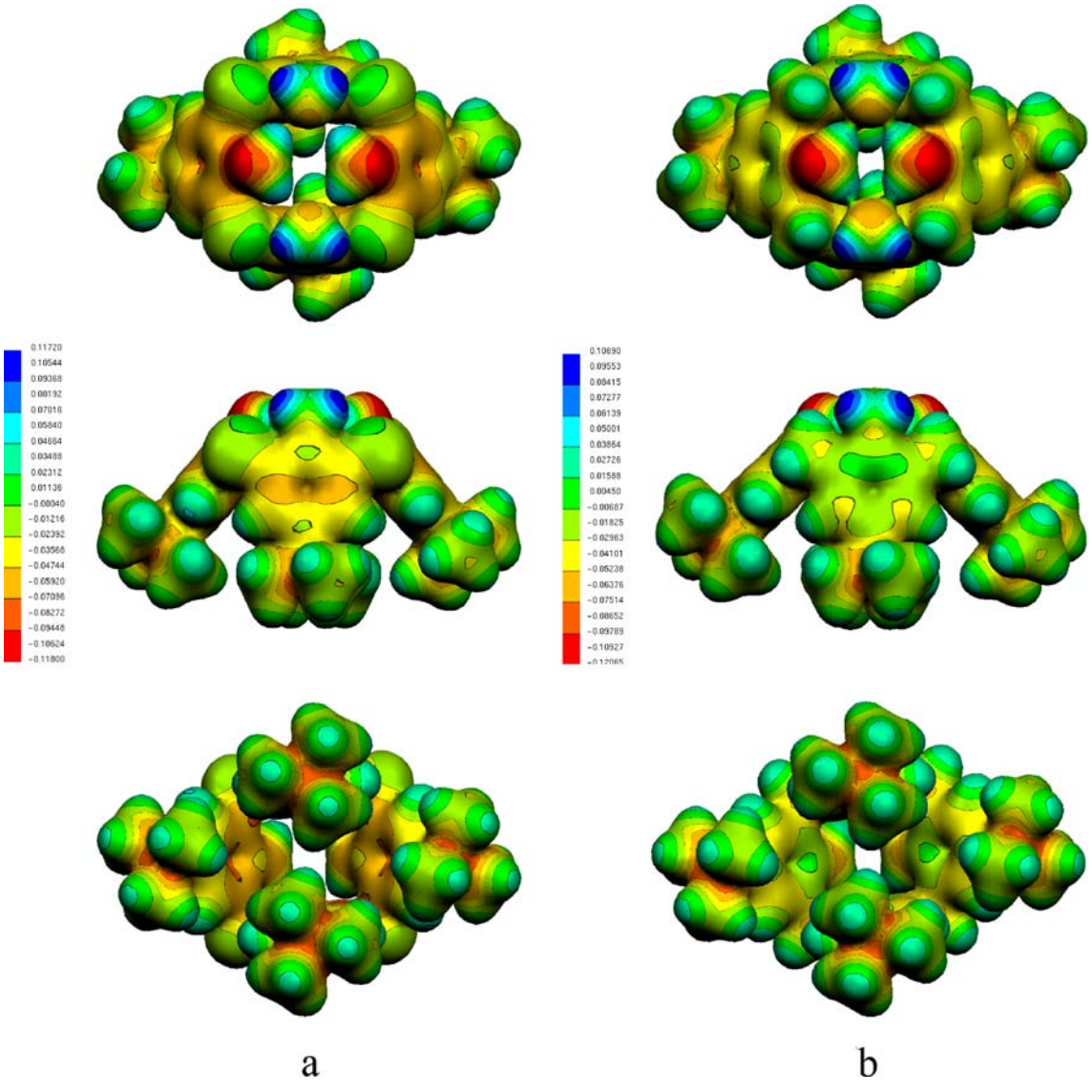

Fig. 7 Top, side, and bottom views of the molecular electrostatic potential (in au) projected onto the electronic isodensity (ρ=0.015 e Å^{-3}) **a** surface of volume, V_s=404.60 Å^3, minimum, ψ_- and maximum, ψ_+ potentials of ψ_-=−0.1180 and ψ_+=0.1172 for tetraamino-*tert*-butylthiacalix[4]arene (tatbtc4a) and **b** V_s=398.20 Å^3, ψ_-=−0.1206 and ψ_+=0.1069 for tetraamino-*tert*-butylcalix [4]arene (tatbc4a)

which is stabilized by −67.61 kcal mol^{-1}. The stability of the tatbtc4a/carboxylate complex system in decreasing order is: oxalate > malonate > succinate > glutarate > pimelate >> acetate. The ONIOM(B3LYP/6-31G(d):AM1)-optimized geometries of the tatbc4a complexes with carboxylate guests are show in Fig. 6. Figure 6 shows that the geometries of malonate/tatbc4a and succinate/tatbc4a complexes have C_2 symmetry. Table 6 also shows large changes in the preorganization energies for the host molecules (>30 kcal mol^{-1} except for the acetate ion, whose energy is 19.27 kcal mol^{-1}), and the small changes for all guests except adipate and pimelate. The total preorganization energies of all the tatbc4a complexes are higher than 45 kcal mol^{-1} except for the acetate ion (19.94 kcal mol^{-1}). The adipate/tatbc4a complex is destabilized by its total preorganization energies ($\Delta E^{total}_{preorg.}$ =113.9 kcal mol^{-1}) (see Table 6). Plots of the preorganization energies of tatbc4a and its complexation and binding energies against the size of carboxylate guests, based upon the ONIOM(B3LYP/6-31G(d):AM1) method, are shown in Fig. 5b.

The BSSE-corrected energies of the tatbc4a complexes computed at the B3LYP/6-31G(d)//ONIOM(B3LYP/6-31G(d):AM1) level (shown in Table 7) confirm that the oxalate ion forms the most stable complex with the tatbc4a receptor. According to the B3LYP/6-31G(d)//ONIOM (B3LYP/6-31G(d):AM1)-energy with and without BSSE corrections, the stability of the tatbtc4a complexes in decreasing order is: oxalate > malonate > succinate > glutarate > adipate > pimelate.

Electronic potential surfaces

Electrostatic potential surfaces of the tatbtc4a and tatbc4a were generated from the Gaussian output files of their B3LYP/6-31G(d) computation with the GFPRINT and POP=FULL keywords using the MOLEKEL 4.3 program [28]. The electrostatic potential (in au) projected onto the electronic isodensity (ρ=0.015 e Å^{-3}) surface of volume, V_s=404.60 Å^3, minimum (ψ_-) and maximum (ψ_+) potentials of ψ_-=−0.1180 and ψ_+=0.1172 for the tatbtc4a and V_s=398.20 Å^3, ψ_-=−0.1206 and ψ_+=0.1069 for the tatbc4a are shown in Fig. 7. The color maps of electronic isodensity surfaces of tatbtc4a and tatbc4a in Fig. 7 show strong positive charge on the amino protons of the two opposite amino groups and strong negative charges on the amino nitrogen atoms on the other amino groups. The positive charges of the amino protons on the tatbtc4a are stronger than those on tatbc4a. Because of the positive charges on amino protons, both of the tatbtc4a and tatbc4a are able to form complexes with the appropriate carboxylate anions, such as malonate and oxalate. Although the localization of the LUMO and HOMO orbitals in the two receptors (tatbtc4a and tatbc4a), as shown in Fig. 8, are nearly the same shape, their HOMO–LUMO energy gaps $\Delta E_{\text{HOMO–LUMO}}$ are quite different; $\Delta E_{\text{HOMO–LUMO}}$ for tatbtc4a and tatbc4a are 4.48 and 4.66 eV, respectively. As the HOMO–LUMO energy gap of tatbtc4a is smaller than that of tatbc4a, tatbtc4a should be able to form more stable complexes than tatbc4a. This is indicated by the binding energies of the malonate complexes, of which the binding energies are −117.60 and −64.09 kcal mol^{-1} for the tatbtc4a and tatbc4a receptors, respectively.

Atomic charges of the binding atoms of the three most stable complexes of tatbtc4a and tatbc4a interacting with carboxylate guests and their hydrogen bond distances

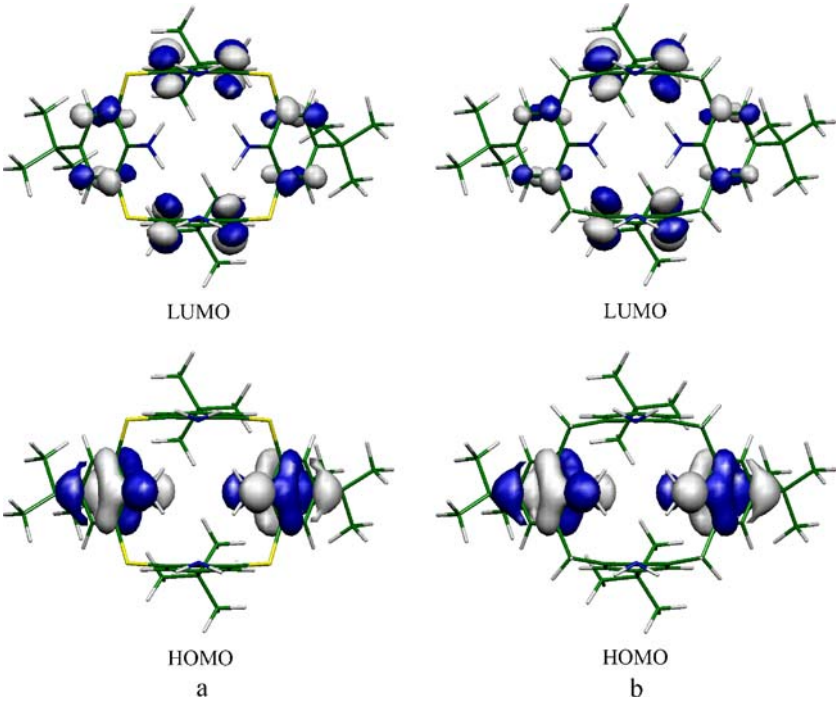

Fig. 8 Localization of the LUMO (*above*) and HOMO (*bottom*) orbitals in **a** tetraamino-*tert*-butylthiacalix[4]arene (tatbtc4a) and **b** tetraamino-*tert*-butylcalix[4]arene (tatbc4a)

Table 8 Atomic charges of binding atoms (treated as high layer) of three most stable complexes of tatbtc4a and tatbc4a with carboxylate guests and hydrogen bond distances obtained by the ONIOM(B3LYP/6-31G(d):AM1) calculations

Properties/host–guest	tatbtc4a			tatbc4a		
	Acetate	Oxalate	Malonate	Acetate	Oxalate	Malonate
Host's atomic charges[a]						
S1	–	–	–	−0.084	−0.089	−0.074
S2	–	–	–	−0.079	−0.054	−0.067
S3	–	–	–	−0.056	−0.052	−0.074
S4	–	–	–	−0.043	−0.102	−0.067
N1	−0.622	−0.650	−0.648	−0.677	−0.577	−0.678
N2	−0.676	−0.741	−0.805	−0.602	−0.797	−0.782
N3	−0.621	−0.778	−0.649	−0.660	−0.718	−0.678
N4	−0.675	−0.776	−0.805	−0.737	−0.780	−0.782
H1	0.170	0.243	0.233	0.307	0.195	0.267
H2	0.276	0.235	0.241	0.205	0.267	0.260
H3	0.274	0.252	0.293	0.217	0.197	0.299
H4	0.200	0.292	0.288	0.216	0.364	0.301
H5	0.169	0.273	0.233	0.208	0.270	0.267
H6	0.276	0.299	0.241	0.294	0.288	0.260
H7	0.274	0.307	0.293	0.257	0.351	0.299
H8	0.177	0.263	0.289	0.292	0.230	0.301
Guest's atomic charges[a]						
O1	−0.633	−0.679	−0.636	−0.624	−0.666	−0.628
O2	−0.628	−0.637	−0.634	−0.613	−0.595	−0.630
O3	–	−0.681	−0.634	–	−0.637	−0.628
O4	–	−0.664	−0.636	–	−0.633	−0.630
Hydrogen bond distance[b]						
O1–H8 (O1–H6)	(1.876)	(1.896)	(1.963)	1.883	(1.857)	(1.955)
O1–H7(O1–H1)	2.005	1.777	1.955	(1.889)	1.732	2.003
O2–H6 (O2–H4)[O2–H2]	[1.881]	–	(1.981)	1.969	–	(1.994)
O2–H7 (O2–H5)[O2–H3]	[2.011]	–	(2.008)	2.119	–	(1.912)
O3–H1	–	2.896	2.008	–	2.685	1.912
O3–H2 (O3–H8)	–	1.976	(1.981)	–	2.039	(1.994)
O4–H3 (O4–H5)	–	(1.967)	1.955	–	(1.927)	2.003
O4–H4 (O4–H2)	–	1.631	(1.962)	–	1.566	(1.955)

[a]In au
[b]In Å, values in parenthesis and bracket belong to their bond distances in corresponding parentheses

computed at the ONIOM(B3LYP/6-31G(d):AM1) level are listed in Table 8. All the binding atoms shown in Table 8 were treated as the high-level layer of the ONIOM (B3LYP/6-31G(d):AM1) model (see Fig. 2).

Conclusions

The preorganization and binding energies of the receptors tatbtc4a and tatbc4a and seven carboxylate guests (acetate, oxalate, malonate, succinate, glutarate, adipate, and pimelate) and complexation energies of their complexes were obtained using the ONIOM (B3LYP/6-31G(d):AM1) and B3LYP/6-31G(d)//ONIOM(B3LYP/6-31G(d):AM1) methods. Thermodynamic quantities, preorganization energies, and complexation energies of these complexes were computed at the ONIOM (B3LYP/6-31G(d):AM1) level of theory. The relative stability of the tatbtc4a complexes with carboxylates in decreasing order is malonate > oxalate > succinate > glutarate. The relative stability of the tatbc4a complexes with carboxylates in decreasing order is oxalate > malonate > succinate > glutarate > adipate > pimelate. The complexes tatbtc4a/malonate and tatbc4a/oxalate were found to be the most stable species. The selectivity of the tatbtc4a receptor toward to malonate with respect to oxalate, in terms of selectivity coefficient, $K^{oxalate}_{malonate}$ is 9.90×10^{2}.

Acknowledgements The authors gratefully acknowledge the Thailand Research Fund for financial support (grant no. BRG4680011). The Rachadapisek Sompoch Endowment Fund, Chulalongkorn University is acknowledged for providing infrastructure facilities.

References

1. Kato R, Nishizawa S, Hayashita T, Teramae N (2001) Tetrahedron Lett 42:5053–5056
2. Lee DH, Lee KH, Hong J-I (2001) Org Lett 3:5–8
3. Lee DH, Lee HY, Lee KH, Hong J-I (2001) Chem Commun 1188–1189
4. Lee DH, Lee HY, Hong J-I (2002) Tetrahedron Lett 43: 7273–7276
5. Jiménez D, Martínez-Máñez R, Sancenón F, Soto J (2002) Tetrahedron Lett 43:2823–2825
6. Piatek P, Jurczak J (2002) Chem Commun 20:2450–2451
7. Gunnlaugsson T, Davis AP, OBrien JE, Glynn M (2002) Org Lett 4:2449–2452
8. Fan A, Hong HK, Valiyaveettil S, Vittal JJ (2002) J Supramol Chem 2:247–254
9. Baerrigter H, Grave L, Nissink WM, Chrisstoffels LAJ, Vander Maas JH, Verboom W, de Jong F, Reindoudt DN (1998) Org Chem 63:4174–4180
10. Fan E, Van Arman SA, Kincaid D, Hamilton AD (1993) J Am Chem Soc 115:369–370
11. Lee KH, Hong J-I (2000) Tetrahedron Lett 41:6083–6087
12. Ruangpornvisuti V (2004) J Mol Struct Theochem 686:47–55
13. Wanno B, Sang-aroon W, Tuntulani T, Pulpoka B, Ruangpornvisuti V (2003) J Mol Struct Theorchem 629:137–150
14. Ruangpornvisuti V (2004) J Mol Struct Theorchem 683: 103–113
15. Wanno B, Ruangpornvisuti V (2004) J Mol Struct Theochem 685:57–71
16. Wanno B, Ruangpornvisuti V (2006) J Mol Struct 787:76–89
17. Becke AD (1988) Phys Rev A38:3098–3100
18. Lee C, Yang W, Parr RG (1988) Phys Rev B37:385–789
19. Maseras F, Morokuma K (1995) J Comput Chem 16: 1170–1179
20. Humbel S, Sieber S, Morokuma K (1996) J Chem Phys 105:1959–1967
21. Dewar MJS, Reynolds CH (1986) J Comput Chem 2:140–143
22. Stewart JJP (1989) Comput Chem 10:209–220
23. Dewar MJS, Thiel W (1977) J Am Chem Soc 99:4899–4907
24. Dapprich S, Komaromi I, Byun KS, Morokuma K, Frisch MJ (1999) J Mol Struct Theochem 461:1–21
25. Remko M, Walsh OA, Richards WG (2001) J Phys Chem A 105:6926–6931
26. Remko M (2002) J Phys Chem A 106:5005–5010
27. Frisch MJ, Trucks GW, Schlegel HB, Scuseria GE, Robb MA, Cheeseman JR, Montgomery JAJr, Vreven T, Kudin KN, Burant JC, Millam JM, Iyengar SS, Tomasi J, Barone V, Mennucci B, Cossi M, Scalmani G, Rega N, Petersson GA, Nakatsuji H, Hada M, Ehara M, Toyota K, Fukuda R, Hasegawa J, Ishida M, Nakajima T, Honda Y, Kitao O, Nakai H, Klene M, Li X, Knox JE, Hratchian HP, Cross JB, Adamo C, Jaramillo J, Gomperts R, Stratmann RE, Yazyev O, Austin AJ, Cammi R, Pomelli C, Ochterski JW, Ayala PY, Morokuma K, Voth GA, Salvador P, Dannenberg JJ, Zakrzewski VG, Dapprich S, Daniels AD, Strain MC, Farkas O, Malick DK, Rabuck AD, Raghavachari K, Foresman JB, Ortiz JV, Cui Q, Baboul AG, Clifford S, Cioslowski J, Stefanov BB, Liu G, Liashenko A, Piskorz P, Komaromi I, Martin RL, Fox DJ, Keith T, Al-Laham MA, Peng CY, Nanayakkara A, Challacombe M, Gill PMW, Johnson B, Chen W, Wong MW, Gonzalez C, Pople JA (2003) Gaussian 03, Revision B.03. Gaussian Inc, Pittsburgh PA
28. Flükiger P, Lüthi HP, Portmann S, Weber J (2000) MOLEKEL 4.3. Swiss Center for Scientific Computing, Manno, Switzerland
29. Boys SF, Bernadi F (1970) Mol Phys 19:553–566
30. Mayer I, Surjan PR (1992) Chem Phys Lett 191:497–499
31. Turi L, Dannenberg JJ (1993) J Phys Chem 97:2488–2490
32. Simon S, Duran M, Dannenberg JJ (1999) J Phys Chem A 103:1640–1643
33. Hamza A, Vibok A, Halasz GJ, Mayer I (2000) J Mol Struct Theochem 427:501–502
34. Makowski M, Raczyska ED, Chmurzyski L (2001) J Phys Chem A 105:869–874
35. Long Y, Liu Y, Lei L, Nie L, Yao S (2001) Analyst 126: 1090–1094